SINTEF
PROCEEDINGS
2

Proceedings of the 12th International Conference on Computational Fluid Dynamics in the Oil & Gas, Metallurgical and Process Industries

Progress in Applied CFD – CFD2017

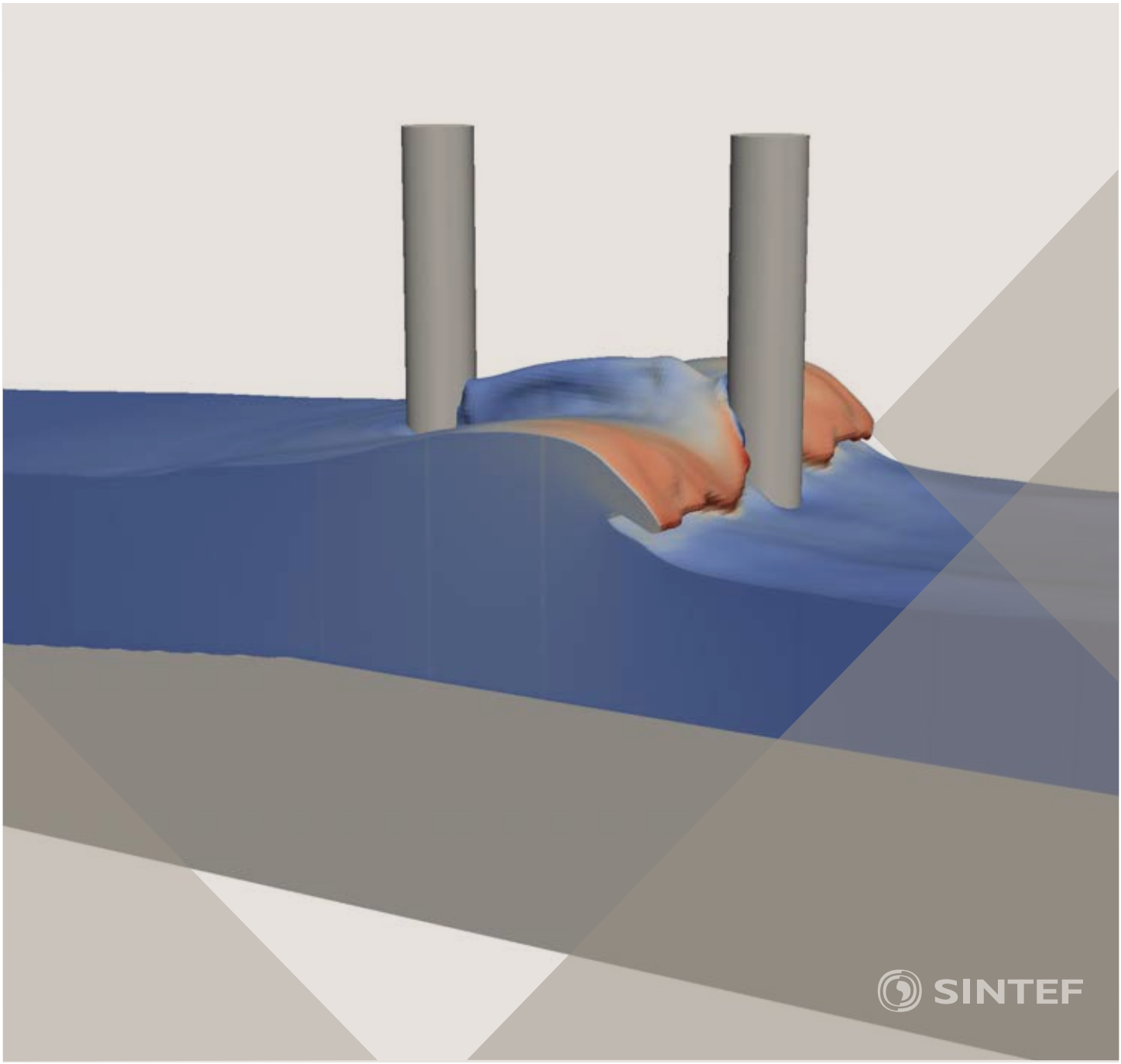

SINTEF Proceedings

Editors:
Jan Erik Olsen and Stein Tore Johansen

Progress in Applied CFD – CFD2017

Proceedings of the 12th International Conference on Computational Fluid Dynamics in the Oil & Gas, Metallurgical and Process Industries

SINTEF Academic Press

SINTEF Proceedings no 2
Editors: Jan Erik Olsen and Stein Tore Johansen
Progress in Applied CFD – CFD2017
Selected papers from 10th International Conference on Computational Fluid Dynamics in the Oil & Gas, Metallurgical and Process Industries

Key words:
CFD, Flow, Modelling

Cover, illustration: Arun Kamath

ISSN 2387-4295 (online)
ISBN 978-82-536-1544-8 (pdf)

SINTEF Academic Press
Address: Forskningsveien 3 B
PO Box 124 Blindern
N-0314 OSLO
Tel: +47 73 59 30 00
Fax: +47 22 96 55 08

www.sintef.no/byggforsk
www.sintefbok.no

SINTEF Proceedings
SINTEF Proceedings is a serial publication for peer-reviewed conference proceedings on a variety of scientific topics.
The processes of peer-reviewing of papers published in SINTEF Proceedings are administered by the conference organizers and proceedings editors. Detailed procedures will vary according to custom and practice in each scientific community.

PREFACE

This book contains all manuscripts approved by the reviewers and the organizing committee of the 12th International Conference on Computational Fluid Dynamics in the Oil & Gas, Metallurgical and Process Industries. The conference was hosted by SINTEF in Trondheim in May/June 2017 and is also known as CFD2017 for short. The conference series was initiated by CSIRO and Phil Schwarz in 1997. So far the conference has been alternating between CSIRO in Melbourne and SINTEF in Trondheim. The conferences focuses on the application of CFD in the oil and gas industries, metal production, mineral processing, power generation, chemicals and other process industries. In addition pragmatic modelling concepts and bio-mechanical applications have become an important part of the conference. The papers in this book demonstrate the current progress in applied CFD.

The conference papers undergo a review process involving two experts. Only papers accepted by the reviewers are included in the proceedings. 108 contributions were presented at the conference together with six keynote presentations. A majority of these contributions are presented by their manuscript in this collection (a few were granted to present without an accompanying manuscript).

The organizing committee would like to thank everyone who has helped with review of manuscripts, all those who helped to promote the conference and all authors who have submitted scientific contributions. We are also grateful for the support from the conference sponsors: ANSYS, SFI Metal Production and NanoSim.

Stein Tore Johansen & Jan Erik Olsen

Organizing committee:

Conference chairman: Prof. Stein Tore Johansen
Conference coordinator: Dr. Jan Erik Olsen
Dr. Bernhard Müller
Dr.Sigrid Karstad Dahl
Dr.Shahriar Amini
Dr.Ernst Meese
Dr.Josip Zoric
Dr.Jannike Solsvik
Dr.Peter Witt

Scientific committee:

Stein Tore Johansen, SINTEF/NTNU
Bernhard Müller, NTNU
Phil Schwarz, CSIRO
Akio Tomiyama, Kobe University
Hans Kuipers, Eindhoven University of Technology
Jinghai Li, Chinese Academy of Science
Markus Braun, Ansys
Simon Lo, CD-adapco
Patrick Segers, Universiteit Gent
Jiyuan Tu, RMIT
Jos Derksen, University of Aberdeen
Dmitry Eskin, Schlumberger-Doll Research
Pär Jönsson, KTH
Stefan Pirker, Johannes Kepler University
Josip Zoric, SINTEF

CONTENTS

NUMERICAL SIMULATIONS OF TURBULENT LIQUID-LIQUID DISPERSIONS WITH QUADRATURE-BASED MOMENT METHODS

Antonio BUFFO[1*], **Dongyue LI**[2], **Wioletta PODGÓRSKA**[3], **Marco VANNI**[1], **Daniele L. MARCHISIO**[1]

[1]Department of Applied Science and Technology, Politecnico di Torino, ITALY

[2]Department of Energy Process Engineering and Chemical Engineering, TU Bergakademie Freiberg, Freiberg, GERMANY

[3]Faculty of Chemical and Process Engineering, Warsaw University of Technology, Warsaw, POLAND

[*] E-mail: antonio.buffo@polito.it

ABSTRACT

The accurate description of droplet dynamics in turbulent liquid-liquid dispersions is of great importance in many industrial applications, especially when the economy of the process is determined by the involved mass transfer and chemical reaction rates. In this respect, the proper estimation of the spatial and time evolution of the droplet polydispersity can offer a useful tool to the modeler to design and scale-up relevant processes. In the latest years, computational fluid dynamics (CFD) and population balance modeling (PBM) have been coupled into a single computational tool, paving the way to full-predictive macro-scale models that incorporate sub-models for describing the rate of the relevant phenomena occurring at droplet-scale, such as coalescence, breakage, momentum and mass exchange with the continuous phase. In this work our recent advances on this topic are presented, with a particular attention to two distinct elements: 1) the choice of appropriate coalescence and breakage closures, pointing out the need to account for high-order turbulent phenomena, such as turbulent intermittency through the use of the so-called multifractal formalism; 2) the possibility to carry out simplified spatially homogeneous simulations when there is a clear separation of scales between coalescence/breakage and mixing. CFD simulations were carried out with our own implementation of the Quadrature Method of Moments (QMOM), combined with the two-fluid model, present in a solver of the open-source code OpenFOAM.

Keywords: Population Balance Methods, droplet dynamics, Multiphase heat and mass transfer, stirred tanks .

INTRODUCTION

Turbulent polydisperse liquid-liquid systems, where droplets are immersed in a continuous liquid phase, are very common in several industrial applications, such as: cosmetic, pharmaceutical, oil and gas, polymer and food industries. Such dispersions are often generated in stirred tanks, where the power input is given to enhance mass, momentum and energy transfer rates between the phases in the desired processes (e.g., polymerization, extraction, separation and emulsification). The most important properties of the system to characterize is the droplet size distribution (DSD), as the dispersion stability, rheological properties and mass transfer rate strongly depend on it. The disperse droplets undergo coalescence and breakage causing changes in the DSD, which are known to depend on the geometry of the tank, the operating conditions and locally within the tank (Alopaeus *et al.*, 2009). In fact, droplets break-up mostly occurs in the region close to the impeller, shifting the DSD towards smaller diameters, while coalescence likely takes place in the stagnant zones far from the impeller, skewing the DSD towards larger diameters.

In this context, the use of a computational tool capable of predicting the complex interaction between the phases can help the design and scale-up of liquid-liquid stirred tanks. The evolution of the DSD in space and time is often related with the flow field, and computational fluid dynamics (CFD) is nowadays commonly use to obtain such information. Moreover, CFD is often coupled with population balance models (PBM) to predict the evolution of the DSD and other properties of the dispersion. In the latter works, CFD-PBM models are used to simultaneously consider the flow inhomogeneities and the DSD evolution. However, there are still two main challenges related to this approach that still need to be addressed: the improvement of the computational efficiency of these calculations, through problem simplification, and the accuracy of the sub-models accounting for breakage and coalescence.

Regarding the first aspect, simplified approaches where the PBM is decoupled from the fluid dynamics description are often used, by prescribing for an entire vessel single volume-averaged values of the relevant properties, used to model the phenomena involved (e.g., coalescence, breakage and mass transfer). These "lumped" models usually stem on the volume-average turbulent dissipation rate, calculated from the stirring power input per unit mass, or estimated through correlations (Attarakih *et al.*, 2008, 2015; Bhole *et al.*, 2008). Although the solution methods in these cases is very fast from the computational point of view, these simplified approaches can be used only under certain conditions. In fact, simulation results obtained with detailed models, accounting for the detailed hydrodynamics under turbulent conditions, may significantly differ from the ones obtained with simplified models, where fluid dynamics homogeneity (and thus homogeneous distribution of all the properties of interest) is imposed (Marchisio *et al.*, 2003, 2006; Vanni and Sommerfeld, 1996).

As far as the second aspect is concerned, the modelling of droplet coalescence and breakage is the subject of many studies. One of the pioneering works on this topic, and still nowadays very popular for its simplicity, is the application of the Kolmogorov turbulence theory by Coulaloglou and Tavlarides (1977). They used the statistical theory of tur-

bulence to derive the coalescence and breakage kernels; the same methodology was also applied by many others (Luo and Svendsen, 1996; Alopaeus *et al.*, 2002; Laakkonen *et al.*, 2007) to derive new and improved kernels. In this context, the developed kernels were also tested using multi-block (compartment) models, not only for liquid-liquid dispersions but also for gas-liquid (bubbly) systems. However, some important factors influencing the droplet coalescence and breakage rates, such as the disperse phase viscosity and turbulence intermittency, are neglected in the CT kernels. Based on the multifractal theory of turbulence, Baldyga and Podgórska (1998) and Podgorska and Baldyga (2001) derived new breakage and coalescence kernels, the so-called "multifractal " (MF) kernels, which include the effect of both disperse phase viscosity and turbulence intermittency.

In this work, we investigated both aspects. First, we formulated a consistent framework to derive and solve the governing equations for zero-dimensional (0D) "lumped" models (where the volume-averaged turbulent dissipation rate is used), 0D "homogeneous" models (where the volume-distribution of the turbulent dissipation rate is considered instead) and three-dimensional (3D) spatially inhomogeneous models (where CFD-PBM model is used). The comparison between these three different approaches is here performed through the investigation of the very same system, in order to point out the conditions (if any) where the 3D inhomogeneous model does not give any additional insight in the characterization of the system, offering the modeler the possibility to use simple 0D models and save computational time and resources. Then, we focused on the CFD-PBM model, by implementing and validating the MF coalescence and breakage kernels through comparison with experimental data. Our implementation of QMOM was employed to solve a PBM in the CFD code OpenFOAM-2.2.x to simulate turbulent liquid-liquid dispersions. The kernels developed by Coulaloglou and Tavlarides (1977) and by Baldyga and Podgórska (1998) and Podgorska and Baldyga (2001) were both employed and compared with the experimental data available.

MODEL DESCRIPTION

Three dimensional (3D) CFD-PBM model

The two-fluid model (TFM) is the CFD framework where PBM is implemented. In this model, both continuous and disperse phases are described by means of the definition of their volume fraction and other average field variables (such as momenta and enthalpies). The governing equations are here not reported for the sake of brevity, however the reader may refer to our previous works for a detailed discussion (Buffo and Marchisio, 2014; Buffo *et al.*, 2016a).

An important element of the CFD-PBM is the modeling of the momentum exchange between the phases, as this term takes into account the coupling between the DSD evolution and the fluid dynamics behavior of the system. In the present work, the only forces considered are gravity, buoyancy and drag. This simplification is possible for turbulent liquid-liquid stirred tanks, since the flow field is mainly determined by the motion of the stirrer. The drag force per unit volume can be estimated by means of the following equation:

$$\mathbf{F}_{\text{drag}} = \alpha_{\text{d}}\alpha_{\text{c}}\left(\frac{3}{4}C_{\text{D}}\frac{\rho_{\text{d}}}{d_{32}}\left|\mathbf{U}_{\text{r}}\right|\right)\mathbf{U}_{\text{r}}, \tag{1}$$

where $\mathbf{U}_{\text{r}} = \mathbf{U}_{\text{c}} - \mathbf{U}_{\text{d}}$, $\mathbf{U}_{\text{c}}$ and $\mathbf{U}_{\text{d}}$ are respectively the average velocity of the continuous and disperse phases, d_{32} is the mean Sauter diameter of the droplets calculated through the PBM, α_{d} is the volume fraction of the disperse phase and α_{c} is that of the continuous phase and C_{D} is the drag coefficient, calculated here through the Schiller and Naumann (1935) correlation.

The turbulence is here described through a RANS model, namely a multiphase extension of the $k-\varepsilon$ model is adopted: only two equations written in terms of the turbulent kinetic energy k and turbulent dissipation rate ε of the continuous phase are solved. Although a certain turbulent anisotropy can be observed in stirred tank reactors operating at high Reynolds numbers, the RANS model based on homogeneous isotropic turbulence theory, represents the only feasible option for the simulation of large scale liquid-liquid systems, since it is a good compromise between computational costs and accuracy.

The CFD-PBM involves also the solution of the so-called Population Balance Equation (PBE). As previously mentioned, the method used to solve the equation is the Quadrature Method of Moments (QMOM). The general idea behind QMOM is to approximate the unknown DSD, $n(\xi)$, by a summation of Dirac delta functions (Marchisio and Fox, 2013):

$$n(\xi) \approx \sum_{\alpha=1}^{N} w_\alpha \delta(\xi - \xi_\alpha), \tag{2}$$

where w_α and ξ_α are the N weights and nodes of the quadrature approximation of order N and of course ξ is the droplet size. As well known the N nodes and weights are calculated in QMOM from the first $2N$ moments of the DSD:

$$M_k = \int_0^\infty n(\xi)\xi^k \mathrm{d}\xi \approx \sum_{\alpha=1}^{N} w_\alpha \xi_\alpha^k, \tag{3}$$

with $k \in 0,\ldots,2N-1$, by using the so-called moment inversion algorithms, such as for example the Product-Difference and Wheeler algorithms (Marchisio and Fox, 2013). The moments of the DSD are, in turn, calculated by solving the following transport equations:

$$\frac{\partial M_k}{\partial t} + \nabla\cdot(\mathbf{U}_{\text{d}} M_k) = \overline{S}_k, \tag{4}$$

again with $k \in 0,\ldots,2N-1$, derived by applying the moment transform to the PBE. By using the quadrature approximation, the source term of Eq. (4) can be written as:

$$\overline{S}_k \approx \frac{1}{2}\sum_{\alpha=1}^{N}\sum_{\beta=1}^{N} w_\alpha w_\beta a_{\alpha,\beta}\left[\left(\xi_\alpha^3 + \xi_\beta^3\right)^{k/3} - \xi_\alpha^k - \xi_\beta^k\right] + \sum_{\alpha=1}^{N} w_\alpha g_\alpha\left(\overline{b}_\alpha^k - \xi_\alpha^k\right), \tag{5}$$

where $a_{\alpha,\beta} = a(\xi_\alpha,\xi_\beta)$ is the coalescence kernel, $g_\alpha = g(\xi_\alpha)$ is the breakage kernel and:

$$\overline{b}_\alpha^k = \int_0^\infty \xi^k \beta(\xi|\xi_\alpha)\,\mathrm{d}\xi. \tag{6}$$

is the generic order moment of the daughter distribution function $\beta(\xi|\xi_\alpha)$. For further details on the corresponding mathematical theory, the reader is referred to the work of Marchisio and Fox (2013).

Zero dimensional (0D) models

As previously mentioned, the DSD and all the other relevant properties in a stirred tank depend of the spatial coordinates and time. However, under certain limited operating conditions, the system can be considered as homogeneous and the evolution of the system can be described in terms of a volume-averaged DSD:

$$\bar{n}(t;\xi) = \frac{1}{V}\int_V n(t,\mathbf{x};\xi)\mathrm{d}\mathbf{x}, \tag{7}$$

where the volume averaging procedure is performed over the entire vessel with volume V. The volume-averaged PBE can be derived by applying the same averaging procedure and the mathematical details are here omitted for the sake of brevity (for a thorough discussion the reader may refer to Buffo *et al.*, 2016b). Here it is important to point out that the the source term of the PBE depends not only on the DSD, but also on the turbulent dissipation rate, which presents a strong spatial inhomogeneity in stirred vessel. Therefore we can leave out the spatial dependency of the turbulent dissipation rate, $\varepsilon = \varepsilon(\mathbf{x})$, resulting in the following expression for the volume-averaged source term of the PBE:

$$\frac{\partial \bar{n}(t,\xi)}{\partial t} = \frac{1}{V}\int_V S(t,\mathbf{x},\xi)\mathrm{d}\mathbf{x} = \int_0^{+\infty} S(t,\varepsilon,\xi)\, f(\varepsilon)\mathrm{d}\varepsilon = \bar{S}(t,\xi), \tag{8}$$

where $f(\varepsilon)$ is the turbulent dissipation rate distribution in the stirred tank so that: $f(\varepsilon)\mathrm{d}\varepsilon$, represents the volume fraction of fluid in the tank which experiences a turbulent dissipation rate between ε and $\varepsilon + \mathrm{d}\varepsilon$. Then, by definition:

$$\int_0^{+\infty} f(\varepsilon)\mathrm{d}\varepsilon = 1, \qquad \int_0^{+\infty} f(\varepsilon)\varepsilon\mathrm{d}\varepsilon = \bar{\varepsilon}, \tag{9}$$

where $\bar{\varepsilon}$ is the volume-average turbulent dissipation rate in the tank. In fact, even if very intense mixing smooths out all the gradients of the DSD, allowing for the approximation of the DSD with its corresponding volume-averaged $\bar{n}(t,\xi)$, the source term may still depend on the spatial coordinate because of the turbulent dissipation rate, $\varepsilon = \varepsilon(\mathbf{x})$, through the term representing the turbulent dissipation rate distribution in the stirred tank $f(\varepsilon)$. This modeling approach is referred as 0D "homogeneous" model and it can be used to replace the 3D CFD-PBM model when the DSD is spatially uniform.
Due to the non-linear dependency on the turbulent dissipation rate of the coalescence and breakage kernels, as we will see in the following paragraph, the 0D "homogeneous" model differs from the 0D "lumped" model, where the kernels are simply evaluated with the volume-averaged value of the turbulent dissipation rate, $\bar{\varepsilon}$. In this latter case, the averaging procedure leads to the following volume-averaged PBE:

$$\frac{\partial \bar{n}(t,\xi)}{\partial t} = \frac{1}{V}\int_V S(t,\mathbf{x},\xi)\mathrm{d}\mathbf{x} = \bar{S}(t,\bar{\varepsilon},\xi). \tag{10}$$

For a detailed derivation of the governing equations, the reader may refer to Buffo *et al.* (2016b) for further details.

Coalescence and breakage kernels

Two different sets of kernels are used in this study to describe droplet breakage and coalescence: the Coulaloglou and Tavlarides (1977) (CT) kernels and the Baldyga and Podgórska (1998); Podgorska and Baldyga (2001) or multifractal (MF) kernels.

CT kernels

Coulaloglou and Tavlarides (1977) proposed a breakage frequency model that takes into account the oscillations of the droplet surface caused by turbulent eddies. The breakage kernel reads as follows:

$$g_{\mathrm{CT}}(\xi) = G_1 \frac{\varepsilon^{1/3}}{\xi^{2/3}} \exp\left(-G_2 \frac{\sigma}{\rho_c \varepsilon^{2/3}\xi^{5/3}}\right), \tag{11}$$

where ε is the turbulent energy dissipation rate, ξ is the droplet diameter, ρ_c is the density of the continuous phase and σ is the interfacial tension. G_1 and G_2 are dimensionless constants, typically derived by fitting with experiments and of limited validity. In this work, $G_1 = 0.00481$ and $G_2 = 0.08$, as suggested in the literature (Liao and Lucas, 2009) and as done in our previous work (Gao *et al.*, 2016).
Coalescence is instead determined by turbulent-induced collisions, that can be quantified through the homogeneous turbulence theory. Then a coalescence efficiency should be considered as not all the collisions will result in coalescence: this term is usually calculated as the exponential of the ratio of two characteristic time scales (i.e. film drainage and interaction time scales), resulting in the following coalescence kernel:

$$a_{\mathrm{CT}}(\xi,\xi') = D_1 \varepsilon^{1/3}\left(\xi+\xi'\right)^2\left(\xi^{2/3}+\xi'^{2/3}\right)^{1/2} \exp\left(-D_2 \frac{\mu_c \rho_c \varepsilon}{\sigma^2}\left(\frac{\xi\xi'}{\xi+\xi'}\right)^4\right), \tag{12}$$

where ξ and ξ' are the diameters of the colliding droplets and μ_c is the viscosity of the continuous phase. D_1 is a dimensionless constant of order of magnitude of unity (Liao and Lucas, 2009) and generally taken equal to 0.88. D_2 is another constant and generally fitted with experimental data. In this work, the value of 9×10^{15} m^{-2} was used.

MF kernels

As pointed out by Baldyga and Podgórska (1998), turbulence intermittency, namely the generation of transient and short-lived velocity gradients that result in an intermittent time evolution of the turbulent quantities, may have a great influence on the breakage rate and a non-negligible one on coalescence. Intermittency is usually described through the so-called multi-fractal theory of turbulence, resulting in the following breakage kernel:

$$g_{\mathrm{MF}}(\xi) = C_g \sqrt{\ln\left(\frac{L}{\xi}\right)} \frac{\varepsilon^{1/3}}{\xi^{2/3}} \int_{\alpha_{\min}}^{\alpha_x} \left(\frac{\xi}{L}\right)^{\frac{\alpha+2-3f(\alpha)}{3}} d\alpha, \tag{13}$$

where $C_g = 0.0035$ is derived from the theory. The integral turbulent length scale is calculated as follows: $L = \frac{(2k/3)^{3/2}}{\varepsilon}$, $\alpha_{\min} = 0.12$, whereas the upper bound of multi-fractal exponent α for vigorous eddies, α_x, is given by the following expression:

$$\alpha_x = \frac{2.5\ln\left(\frac{L\varepsilon^{0.4}\rho_c^{0.6}}{C_x \sigma^{0.6}}\right)}{\ln(L/\xi)} - 1.5, \tag{14}$$

where $C_x = 0.23$. Equation (14) is valid only for low viscosity of the disperse phase. The expression for α_x that takes into account viscous effects can be found in Baldyga and Podgórska (1998).

The multi-fractal spectrum has a universal form derived from the experimental data of Meneveau and Sreenivasan (1991):

$$f(\alpha) = a + b\alpha + c\alpha^2 + d\alpha^3 + e\alpha^4 + f\alpha^5 + g\alpha^6 + h\alpha^7 + i\alpha^8, \quad (15)$$

with $a = -3.51, b = 18.721, c = -55.918, d = 120.9, e = -162.54, f = 131.51, g = -62.572, h = 16.1, i = -1.7264$ for $\alpha \geq 0.12$.

Also the MF coalescence kernel is expressed as a product of the coalescence frequency and the coalescence efficiency, this latter expressed as an exponential of drainage time to interaction time ratio resulting in the following relationship (Podgorska and Baldyga, 2001):

$$a_{\mathrm{MF}}(\xi,\xi') = \sqrt{\frac{8\pi}{3}}\varepsilon^{1/3}\left(\frac{\xi+\xi'}{2}\right)^{7/3}\left(\frac{\xi+\xi'}{2L}\right)^{0.027} \times \exp\left(-A_1\frac{t_\mathrm{d}}{t_\mathrm{i}}\right), \quad (16)$$

where ξ and ξ' are the diameters of the colliding droplets and A_1 is a dimensionless coefficient of the order of magnitude unity. In this model, the droplet interfaces are assumed partially mobile, in such a way that the film drainage is controlled by the motion of film surface, in turn controlled by shear stresses exerted on the film by fluid in the drop. Therefore, the drainage time is given as:

$$t_\mathrm{d} = \frac{\mu_\mathrm{d}\tilde{a}R_{\mathrm{eq}}^{3/2}}{4\sigma R_L^{1/2}}\left(\frac{1}{h_c}\left(\frac{\xi^*}{L}\right)^{0.016} - \frac{1}{h_0}\left(\frac{\xi^*}{L}\right)^{-0.01}\right), \quad (17)$$

whereas the interaction time as:

$$t_\mathrm{i} = \frac{1}{2}\left(\frac{8(\rho_\mathrm{d}/\rho_\mathrm{c}+\gamma)\rho_\mathrm{c}R_\mathrm{S}^3}{3\sigma(1+\zeta^3)}\right)^{1/2}. \quad (18)$$

In these two latter equations, γ is the coefficient of virtual mass and L is the integral turbulent length scale. $\xi^* = \frac{\xi+\xi'}{2}$, $\zeta = \frac{R_\mathrm{S}}{R_\mathrm{L}}$, $R_\mathrm{L} = \max(\xi,\xi')/2$ and $R_\mathrm{S} = \min(\xi,\xi')/2$, R_eq is the equivalent radius expressed as: $R_\mathrm{eq} = \frac{\xi\xi'}{\xi+\xi'}$, μ_d is the viscosity of the dispersed phase, $\tilde{a}$ is the film radius derived under the assumption that the whole kinetic energy is transformed into excess surface energy (Podgorska, 2005):

$$\tilde{a} = \left(\frac{8}{3}\frac{(\rho_\mathrm{d}/\rho_\mathrm{c}+\gamma)\rho_\mathrm{c}\varepsilon^{2/3}\xi^{*2/3}R_\mathrm{S}}{\sigma(1+\zeta^3)}\right)^{1/4}(R_\mathrm{S}R_\mathrm{L})^{1/2}. \quad (19)$$

The critical film thickness, h_c, is given by the following expression (Chesters, 1991):

$$h_\mathrm{c} = \left(\frac{AR_\mathrm{eq}}{8\pi\sigma}\right)^{1/3}, \quad (20)$$

where A is the Hamaker constant of the order of magnitude of: $A \approx 10^{-20}$ J, for pure liquid-liquid systems. The initial film thickness, h_0, can be expressed as follows (Podgorska, 2005):

$$h_0 = \frac{\varepsilon^{1/6}\xi^{*1/6}\mu_\mathrm{d}^{1/2}R_\mathrm{eq}^{3/4}\tilde{a}^{1/2}}{2\sigma^{1/2}R_\mathrm{L}^{1/4}}. \quad (21)$$

It is important to remark that A_1 is the model constant that can be fine tuned and, with the fact that appears inside an exponential, model predictions are very sensitive to its value. In fact this constant, although of the order of magnitude of unity from the theory, includes all the modeling uncertainties which might be not of universal character, e.g. the uncertainty related to the Hamaker constant for different liquid-liquid systems.

Daughter size distribution function

The daughter size distribution function $\beta(\xi|\xi')$ is required to describe the droplet breakage event. A detailed discussion on the different daughter distribution functions can be found in the work of Liao and Lucas (2009). In this work, we assumed a binary breakage which is a reasonable assumption for coalescing systems here investigated. In fact, more than two daughter droplets can be detected only when very large droplets break-up (Podgorska, 2006). Therefore, the distribution proposed by Laakkonen *et al.* (2006) is here used:

$$\beta(\xi|\xi') = 180\left(\frac{\xi^2}{\xi'^3}\right)\left(\frac{\xi^3}{\xi'^3}\right)^2\left(1-\frac{\xi^3}{\xi'^3}\right)^2, \quad (22)$$

where ξ and ξ' are the daughter and mother droplets.

Test cases and numerical details

Different simulations were performed in order to investigate the two aspects mentioned earlier. First, a realistic stirred tank reactor with water as the continuous phase and octanol as the disperse phase was considered, for investigating the differences in the results between the 0D "lumped" model, the 0D "homogeneous" model and the 3D CFD-PBM model. Different operating conditions were taken into account, combining different stirring rates of: $N = 300$, 500 and 600 RPM, and different global concentrations of the disperse phase, corresponding to ϕ_d : 0.1 %, 1 % and 10 %.

Then two different sets of coalescence and breakage kernels, namely CT and MF, were used to simulate droplet breakage and coalescence in stirred tanks. Also in this case, different systems and operating conditions were investigated. Test cases correspond to the experimental data from Podgorska (2006, 2007). The time evolution of the volume-averaged mean Sauter diameter of the droplets is available for three different geometries (indicated as T1, T2 and T3), working under different stirring rates and viscosities of the disperse phase. In fact, different silicone oils with viscosity ranging from approximately 1 mPa s to 500 mPa s, and approximately the same interfacial tension were considered. The specific fluid properties, global disperse phase volume fraction, ϕ_d, and stirring rate, N, are reported in Table 1. The geometrical details of the stirred tanks equipped with Rushton turbines for the different geometries investigated are reported in Fig. 1, 2 and 3 .

Table 1: Fluid properties and operating conditions investigated in this work: μ_c is the viscosity of the continuity phase (mPas), μ_d is the viscosity of the dispersed phase (mPas), ρ_c is the density of continuity phase (kg m^{-3}), ρ_d is the density of dispersed phase (kg m^{-3}), σ is the surface tension between the two phases (N m^{-1}), ϕ_d is the global disperse phase volume fraction (-) and N is the impeller rotational speed (rpm).

Geom.	μ_c	μ_d	ρ_c	ρ_d	σ	ϕ_d	N
T1	1.00	0.72	998	1022	0.0250	0.0020	300
T2	1.00	0.72	998	1022	0.0250	0.0020	392
T3	0.89	10.00	997	946	0.0458	0.0038	240
T3	0.89	10.00	997	946	0.0458	0.0038	350
T3	0.89	100.0	997	985	0.0464	0.0038	300
T3	0.89	100.0	997	985	0.0464	0.0038	350
T3	0.89	500.0	997	973	0.0505	0.0038	300
T3	0.89	500.0	997	973	0.0505	0.0038	350

The 0D simulations ("lumped" and "homogeneous" models) of the first part of the work were carried out by means of a

short program written in Matlab. The set of ODEs was integrated by using the standard solver `ode15s`. The initial droplet population is assumed to follow a log-normal distribution with a mean estimated by correlation and standard deviation proportional to that mean.

The 3D simulations were instead performed using our own implementation of QMOM in OpenFOAM (version 2.2.x), that makes use of a modified version of the standard solver `compressibleTwoPhaseEulerFoam` including the transport equation for the moments of the DSD, and the Wheeler inversion algorithm to calculate the quadrature approximation from the transported moments (Buffo *et al.*, 2016a). In this work, only the first six moments of the DSD were calculated ($M_0, M_1, M_2, M_3, M_4, M_5$), corresponding to a quadrature approximation with three nodes: $N = 3$. Particular attention was paid to the problem of moment boundedness and realizability by means of a proper implementation of the moment transport equations (Buffo *et al.*, 2016a). The rotation of the turbine was modelled using the multiple reference frame approach (MRF), which gives reasonable results and is significantly cheaper than the sliding mesh approach.

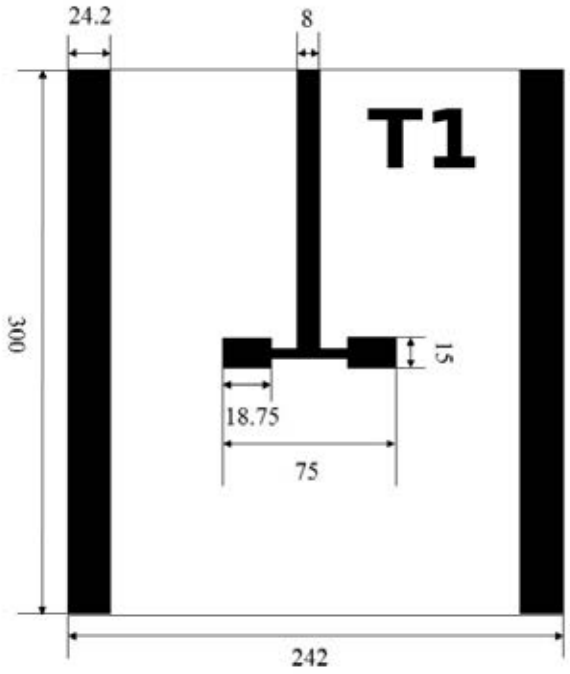

Figure 1: Geometry of the stirred tank T1. The units are in mm.

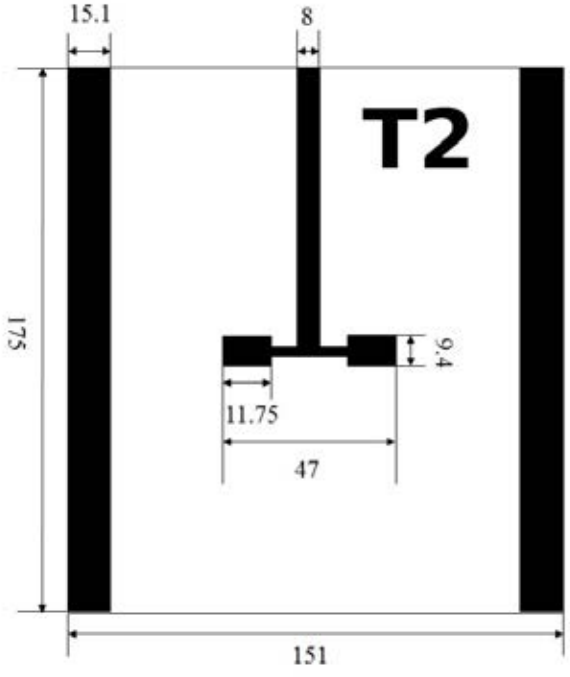

Figure 2: Geometry of the stirred tank T2. The units are in mm.

RESULTS

Let us start the discussion of the results with the comparison of the approximate 0D models with the inhomogeneous 3D models. In Fig. 4 the turbulent dissipation rate distribution in the tank, $f(\varepsilon)$, is shown for the three different stirring rates investigated as estimated from the 3D CFD-PBM model. As can be seen from the figure, at higher stirring rates very high values of ε (up to 135 $m^2\ s^{-3}$) are observed in the region close to the stirrer blade, while in the bulk zone, which represents the major part of the tank volume, much smaller values are observed. At lower impeller rotational speed instead the distribution of ε shows that the turbulence is in general mild, with the values of turbulent dissipation rates concentrated on the left of the plot. It is therefore clear that the volume-averaged kernels for breakage and coalescence, as calculated with the 0D "homogeneous" model, may be significantly different from the kernels evaluated at the volume-average turbulent dissipation rate $\bar{\varepsilon}$, as calculated with the 0D "lumped" model, and this difference will be much more significant with the increase of the rotational speed of the impeller.

It is important to remark that the 0D "homogeneous" model, together with the 3D CFD-PBM model, considers the turbulent dissipation rate distribution in the tank: while, the 3D model has a general validity (as long as all the sub-models for turbulence, drag forces, coalescence and breakage are accurate), the 0D "homogeneous" model is valid only in the case of uniform distribution of the disperse phase throughout the vessel, in such a way that the gradients of all other properties apart from ε can be assumed null. The 0D lumped model, instead, makes use only of the volume-averaged turbulent dissipation rate ε, always neglecting the effect of the

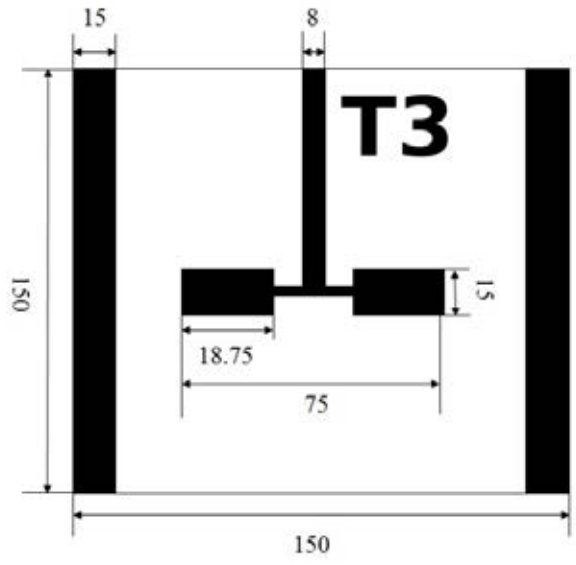

Figure 3: Geometry of the stirred tank T3. The units are in mm.

distribution of turbulent dissipation rate in the tank.

The values of the mean Sauter diameter (d_{32}) at the steady state calculated with the three different methods are reported in Table 2 for two different operating conditions, while Table 3 shows the errors at the steady-state for the mean Sauter diameter as calculated with the 0D "homogeneous" model and the 0D "lumped" model, by using as a reference the predictions of the 3D model for all the different operating conditions investigated. Closer observation of Table 3 shows that 0D "homogeneous" model is able to give predictions that are very close to those given by the 3D CFD-PBM model. It is important to consider the fact that within the range of initial and operating conditions investigated, it was found that breakage always prevailed over coalescence, with the droplet size rapidly decreasing with time, until steady-state

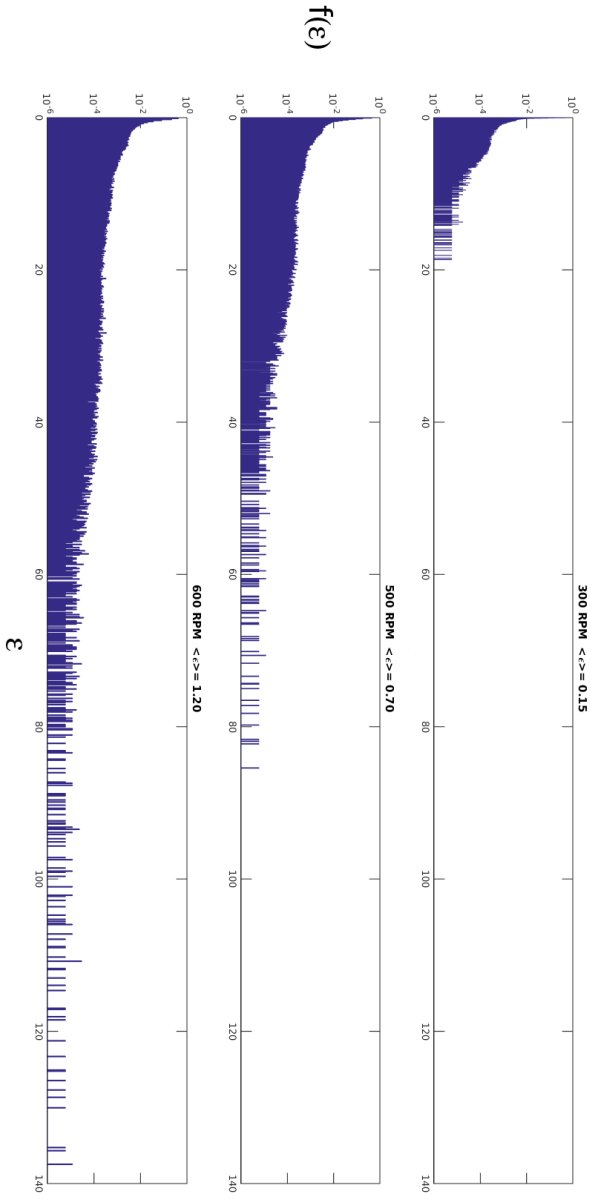

Figure 4: Distribution of the turbulent dissipation rate in the vessel for different operating conditions.

Table 2: Values of the mean Sauter diameter at the steady state for two different operating conditions for all the approaches considered. The units are mm

Approach	300 rpm $\phi_d = 0.1\%$	600 rpm $\phi_d = 10\%$
0D "lumped"	0.239	0.085
0D "homogeneous"	0.046	0.038
3D CFD-PBM	0.047	0.058

Table 3: Difference between mean Sauter diameter calculated with 3D CFD-PBM model and 0D "homogeneous" (normal font) and 0D "lumped" simulations (bold font). Numbers are in percentage.

	RPM					
ϕ_d, %	300		500		600	
0.1	1.7	**249.6**	5.3	**236.3**	8.0	**227.5**
1.0	10.6	**164.7**	12.7	**163.0**	15.0	**159.3**
10.0	20.5	**85.1**	30.0	**65.0**	33.6	**60.0**

was reached. By using the 0D "lumped" model, in some cases of low stirring rate and high disperse phase volume fraction, coalescence prevailed over breakage, since the initial mean droplet diameter is of 1 mm. Moreover, the 0D "lumped" model underestimates the breakage rate in all the investigated cases, independently from the operating conditions, suggesting that this model should not be used even as a simple test case to study in detail the kinetics of coalescence and breakage (or in other words coalescence and breakage kernels) for such systems.

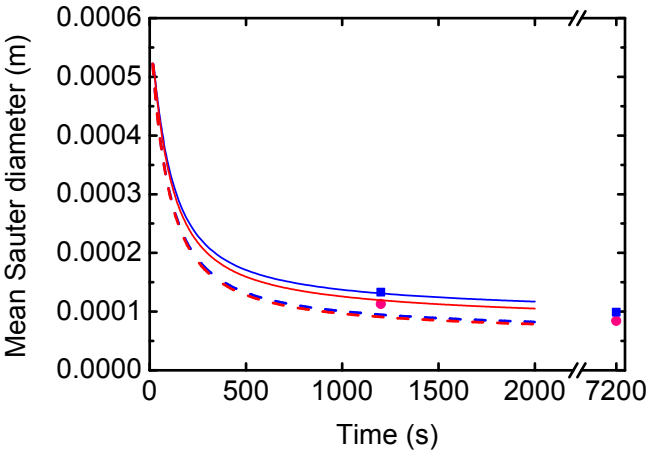

Figure 5: Time evolution of the volume-averaged mean Sauter diameter for T2, $N = 392$ rpm (blue lines) and for T1, $N = 300$ rpm (red lines). Viscosity of the disperse phase equal to 0.72 mPa s

It can be seen also that the 0D "lumped" model produces a very large error, whereas the error associated with the 0D "homogeneous" model is acceptable for some operating conditions. Moreover, it is possible to observe that the error increases both with the stirring rate and the global hold-up of the disperse phase. In particular for $\phi_d = 0.1$ %, the agreement with the reference solution is considerably good. As ϕ_d increases to 1.0 % the agreement for the mean Sauter diameter gets worse. A further increase of the disperse phase hold-up to $\phi_d = 10.0$ % significantly compromise the agreement between the predictions of the 3D CFD-PBM and 0D "homogeneous" models, regardless of the stirring rate. However, this behavior was expected: the 0D "homogeneous" model is in fact applicable only in dilute cases, when the DSD can be

considered uniform throughout the vessel. The error associated with the 0D "lumped" model, instead, is always significant for all the operating conditions investigated, showing

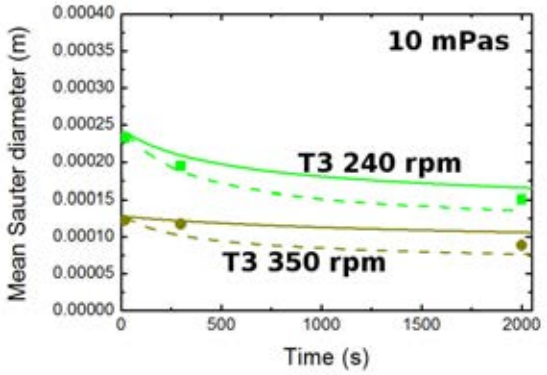

Figure 6: Time evolution of the volume-averaged mean Sauter diameter for T3, $N = 240$ rpm (light green lines) and for T3, $N = 350$ rpm (dark green lines). Viscosity of the disperse phase equal to 10 mPa s.

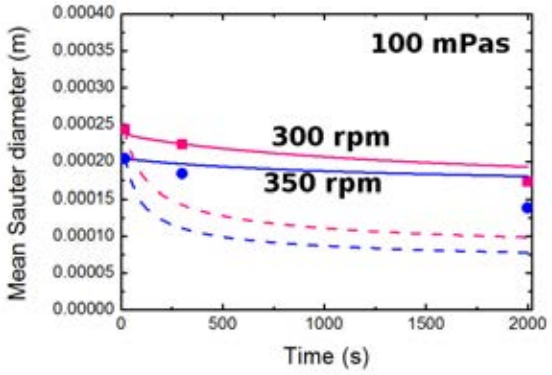

Figure 7: Time evolution of the volume-averaged mean Sauter diameter for T3, $N = 300$ rpm (pink lines) and for T3, $N = 350$ rpm (blue lines). Viscosity of the disperse phase equal to 100 mPa s.

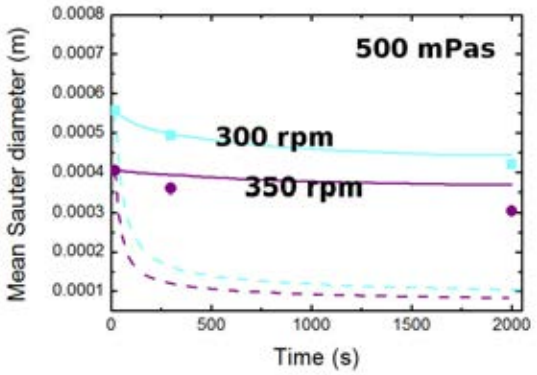

Figure 8: Time evolution of the volume-averaged mean Sauter diameter for T3, $N = 300$ rpm (light blue lines) and for T3, $N = 350$ rpm (purple lines). Viscosity of the disperse phase equal to 500 mPa s.

that the effect of the distribution of turbulent dissipation rate must be properly considered.

As far as the investigation on different sub-models for droplet coalescence and breakage is concerned, it is useful to compare the experimental data available and the numerical predictions in terms of the time evolution of the mean Sauter diameter. As it can be observed different test cases are reported, having different geometries, operating conditions and viscosity of the dispersed phase. It is useful to remind here that experimental data are in general affected by an uncertainty of about 5 %. The sensitivity of model predictions with respect to the key parameters was instead investigated in the cited literature where the kernels were first proposed.

Figure 5 reports the comparison between predictions obtained with the CT kernels (dashed lines) and the MF kernels (continuous lines) for the two stirred tanks, T1 and T2, reported in Figg 1 and 2. T1 is the geometric scale up of T2 and the stirring rates are chosen in order to result with the same power dissipation per unit volume. As seen the CT kernels results in the very same predictions for the mean Sauter diameter, whereas only using the MF kernels a significant difference between the two tanks is observed, in perfect agreement with the experiments. This is due to the effect of intermittency, that is more important in the large tank (T1).

The higher accuracy of the MF kernels is even more evident when the viscosity of the disperse phase is increased up to 10 mPa s, 100 mPa s and 500 mPa s as evident from 6, 7 and 8. In fact, predictions obtained with the MF kernels are close to experiments, whereas those obtained with the CT kernels are not able to reproduce the experimental trend. This is due to the fact that the CT kernels does not take into account the viscous forces that prevent the droplet to break, while the MF kernels properly include this important piece of physics into the model. Moreover, it is worth remarking that the MF kernels are capable of predicting with good accuracy also the dynamics of the investigated systems, which is another significant improvement with respect to the more common CT kernels.

CONCLUSIONS

In this work two different aspects related to the simulation of liquid-liquid systems were considered. First, the predictions of a 3D CFD-PBM model, our own implementation of QMOM in OpenFOAM, were compared with those of two simpler (computationally cheaper and often used in the industrial practice) 0D models, derived from the 3D model with a simple volume-average procedure applied on the entire vessel. The results show that the model which assumes that the turbulence dissipation rate in the tank is uniform and equal to the volume-average value, namely the 0D "lumped" model, is not suitable in all the operating conditions here studied. This is due to the fact that the rates of coalescence and breakage are not homogeneous in the tank, regardless the spatial distribution of the droplet population. Whereas, the 0D "homogeneous" model, which is able to take into account the effect of the spatial distribution of the turbulent dissipation rate in the tank, can be used under certain operating conditions in replacement of the 3D model, when the spatial gradients of the DSD are negligible. This means that the knowledge of the spatial distribution of the turbulent dissipation rate in the tank is crucial for a proper calculation of the breakage and coalescence rates.

Moreover in this work, two different breakage kernels (the CT and the MF kernels) were considered in our simulations. Different test cases were simulated in three geometrically

different tanks working under different operating conditions and with different continuous and disperse phases. Eventually the mean Sauter diameters calculated from the CT kernel and MF kernel were compared with experimental data. The results show that, for dilute systems, the CT and MF kernels both are capable of capturing the evolution of the mean Sauter diameter, however the CT kernel under-predicts the mean Sauter diameter, especially in the case of high disperse phase viscosity, whereas the MF kernels results in satisfactory agreement.

REFERENCES

ALOPAEUS, V., KOSKINEN, J., KESKINEN, K. and MAJANDER, J. (2002). "Simulation of the population balances for liquid-liquid systems in a nonideal stirred tank. Part II: Parameter fitting and the use of the multiblock model for dense dispersions". *Chemical Engineering Science*, **57(10)**, 1815–1825.

ALOPAEUS, V., MOILANEN, P. and LAAKKONEN, M. (2009). "Analysis of stirred tanks with two-zone models". *AIChE Journal*, **55(10)**, 2545–2552.

ATTARAKIH, M., BART, H.J., STEINMETZ, T., DIETZEN, M. and FAQIR, N. (2008). "LLECMOD: A bivariate population balance simulation tool for liquid-liquid extraction columns". *Open Chem. Eng. J*, **2**, 10–34.

ATTARAKIH, M., HLAWITSCHKA, M., ABUKHADER, M., AL-ZYOD, S. and BART, H.J. (2015). "CFD-population balance modelling and simulation of coupled hydrodynamics and mass transfer in liquid extraction columns". *Applied Mathematical Modelling*, **39**, 5105–5120.

BALDYGA, J. and PODGÓRSKA, W. (1998). "Drop break–up in intermittent turbulence: Maximum stable and transient sizes of drops". *The Canadian Journal of Chemical Engineering*, **76**, 456–470.

BHOLE, M., JOSHI, J. and RAMKRISHNA, D. (2008). "CFD simulation of bubble columns incorporating population balance modeling". *Chemical Engineering Science*, **63(8)**, 2267–2282.

BUFFO, A. and MARCHISIO, D. (2014). "Modeling and simulation of turbulent polydisperse gas-liquid systems via the generalized population balance equation". *Reviews in Chemical Engineering*, **30**, 73–126.

BUFFO, A., VANNI, M. and MARCHISIO, D. (2016a). "On the implementation of moment transport equations in OpenFOAM: Boundedness and realizability". *International Journal of Multiphase Flow*, **85**, 223–235.

BUFFO, A., DE BONA, J., VANNI, M. and MARCHISIO, D. (2016b). "Simplified volume-averaged models for liquid-liquid dispersions: Correct derivation and comparison with other approaches". *Chemical Engineering Science*, **153**, 382–393.

CHESTERS, A. (1991). "The modelling of coalescence processes in fluid-liquid dispersions: a review of current understanding". *Chemical Engineering Research and Design*, **69**, 259–270.

COULALOGLOU, C. and TAVLARIDES, L. (1977). "Description of interaction processes in agitated liquid-liquid dispersions". *Chemical Engineering Science*, **32(11)**, 1289–1297.

GAO, Z., LI, D., BUFFO, A., PODGORSKA, W. and MARCHISIO, D. (2016). "Simulation of droplet breakage in turbulent liquid–liquid dispersions with CFD-PBM: Comparison of breakage kernels". *Chemical Engineering Science*, **142**, 277–288.

LAAKKONEN, M., ALOPAEUS, V. and AITTAMAA, J. (2006). "Validation of bubble breakage, coalescence and mass transfer models for gas–liquid dispersion in agitated vessel". *Chemical Engineering Science*, **61**, 218–228.

LAAKKONEN, M., MOILANEN, P., ALOPAEUS, V. and AITTAMAA, J. (2007). "Modelling local bubble size distributions in agitated vessels". *Chemical Engineering Science*, **62(3)**, 721–740.

LIAO, Y. and LUCAS, D. (2009). "A literature review of theoretical models for drop and bubble breakup in turbulent dispersions". *Chemical Engineering Science*, **64**, 3389–3406.

LUO, H. and SVENDSEN, H. (1996). "Theoretical model for drop and bubble breakup in turbulent dispersions". *AIChE Journal*, **42(5)**, 1225–1233.

MARCHISIO, D. and FOX, R. (2013). *Computational models for polydisperse particulate and multiphase systems*. Cambridge University Press.

MARCHISIO, D., VIGIL, R. and FOX, R. (2003). "Implementation of the quadrature method of moments in CFD codes for aggregation-breakage problems". *Chemical Engineering Science*, **58(15)**, 3337–3351.

MARCHISIO, D., SOOS, M., SEFCIK, J. and MORBIDELLI, M. (2006). "Role of turbulent shear rate distribution in aggregation and breakage processes". *AIChE journal*, **52(1)**, 158–173.

MENEVEAU, C. and SREENIVASAN, K. (1991). "The multifractal nature of turbulent energy dissipation". *Journal of Fluid Mechanics*, **224**, 429–484.

PODGORSKA, W. (2005). "Scale–up effects in coalescing dispersions–Comparison of liquid–liquid systems differing in interface mobility". *Chemical Engineering Science*, **60**, 2115–2125.

PODGORSKA, W. (2007). "Influence of dispersed phase viscosity on drop coalescence in turbulent flow". *Chemical Engineering Research and Design*, **85**, 721–729.

PODGORSKA, W. and BALDYGA, J. (2001). "Scale–up effects on the drop size distribution of liquid–liquid dispersions in agitated vessels". *Chemical Engineering Science*, **56**, 741–746.

PODGORSKA, W. (2006). "Modelling of high viscosity oil drop breakage process in intermittent turbulence". *Chemical Engineering Science*, **61**, 2986–2993.

SCHILLER, L. and NAUMANN, A. (1935). "A drag coefficient correlation". *Vdi Zeitung*, **77(318)**, 51–86.

VANNI, M. and SOMMERFELD, M. (1996). "Aggregation of small particles in turbulent liquid flows". *Engineering Turbulence Modelling and Experiments*, **3**, 891–900.